**PRIORITY DOCUMENT**

SUBMITTED OR TRANSMITTED IN
COMPLIANCE WITH RULE 17.1(a) OR (b)

Patent Office
Canberra

REC'D 0 6 JAN 2004

WIPO          PCT

I, JONNE YABSLEY, TEAM LEADER EXAMINATION SUPPORT AND SALES hereby certify that annexed is a true copy of the Provisional specification in connection with Application No. 2003904713 for a patent by COMMONWEALTH SCIENTIFIC AND INDUSTRIAL RESEARCH ORGANISATION as filed on 29 August 2003.

WITNESS my hand this
Twenty-third day of December 2003

JONNE YABSLEY
TEAM LEADER EXAMINATION
SUPPORT AND SALES

# AUSTRALIA

# Patents Act 1990

## Commonwealth Scientific and Industrial Research Organisation

**PROVISIONAL SPECIFICATION**

*Invention Title:*

*Radiographic Equipment*

The invention is described in the following statement:

## Technical Field

This invention concerns radiographic equipment. In particular the invention concerns radiographic equipment for the detection of concealed articles, substances and materials. For instance, the invention may be applied to the detection of concealed

5 weapons, explosives, contraband, drugs and other articles, substances and materials in items such as aircraft baggage, airfreight or shipping containers.

## Background Art

Technologies based on X-rays, gamma-rays and neutrons have been proposed to

10 tackle this problem (Hussein, E., 1992, Gozani, T., 1997, An, J. et al, 2003). The most widely adopted technology is the X-ray scanner which forms an image of an item being examined by measuring the transmission of X-rays through the item from a source to a spatially segmented detector. X-rays are most strongly attenuated by dense, higher atomic number materials such as metals. Consequently, X-ray scanners are ideal for

15 detecting items such as guns, knives and other weapons. However, X-rays provide little discriminating power between organic and inorganic elements. Using X-rays the separation of illicit organic materials such as explosives or narcotics from commonly found, benign organic materials is not possible.

An elemental identification system is being developed for the inspection of

20 commodities shipped on pallets. The system called NELIS (Neutron Elemental Analysis System) utilises a 14 MeV neutron generator and three gamma ray detectors to measure induced gamma rays from the cargo (Dokhale, P.A. et al, 2001; Barzilov, A.P., Womble, P.C. and Vourvopoulos, G., 2001). NELIS is not an imaging system and is used in conjunction with an X-ray scanner to help identify gross composition

25 anomalies.

A Pulsed Fast Neutron Analysis (PFNA) cargo inspection system has been developed (Gozani, T., 1997, Sawa et al., 1991) and commercialised through Ancore Corporation. The PFNA system uses a collimated beam of nanosecond-pulsed fast neutrons and the resulting spectrum of gamma rays is measured. The PFNA method

30 allows the ratios of key organic elements to be measured. The nanosecond-pulsed fast neutrons are required in order to localise the specific regions contributing to the measured gamma-ray signal by time-of-flight spectrometry. In practice the technique is limited by the very expensive and complex particle accelerator, the limited neutron source strength and low gamma-ray detection efficiency and the resulting slow scan

35 speeds.

Neutron radiography systems have the advantage of direct measurement of transmitted neutrons and are therefore more efficient than techniques measuring

secondary radiation such as neutron-induced gamma rays. Fast neutron radiography has the potential to determine the line-of-sight 'organic image' of objects (Klann, 1996). In contrast to X-rays, neutrons are most strongly attenuated by organic materials, especially those with high hydrogen contents.

5      A fast neutron and gamma ray and radiography system has been developed by Rynes et al (1999) to supplement PFNA. In this system nanosecond-pulsed fast neutrons and gamma rays from an accelerator are transmitted through the object and the detected neutron and gamma ray signals are separated by arrival time. The resulting system is claimed to combine the advantages of both X-ray radiography and PFNA

10   systems. However it is limited by the very expensive and complex particle accelerator.

Bartle (1995) has suggested using the fast neutron and gamma-ray transmission technique (Millen et al, 1990) to detect the presence contraband in luggage, etc. However this technique has not been used for imaging and its practical application to contraband detection has not been investigated.

15   Mikerov, V.I. et al, (2000) have investigated the possibility of fast neutron radiography using a 14 MeV neutron generator and luminescent screen/CCD camera detection system. Mikerov found that applications were limited by both the low detection efficiency of the 2 mm thick luminescent screen for fast neutrons and the high sensitivity of the screen to X rays produced by the neutron generator.

20   Neutron radiography systems using a 14 MeV generator and thermal neutron detection are commercially available (Le Tourneur, P., Bach, P. and Dance, W.E., 1998). However the fact that the fast neutrons are slowed down (thermalised) prior to performing radiography limits the size of the object being imaged to a few cm. No fast neutron radiography systems are commercially available that involve fast neutron

25   detection.

Most work conducted with neutron radiography has been conducted in the laboratory using neutrons from nuclear reactors or particle accelerators that are not suited to a freight-handling applications (Lefevre, H.W, et al, 1996, Miller, T.G., 1997, Chen, G. and Lanza, R.C., 2000, Brzosko, J.S. et al, 1992).

30   To improve the ability of fast neutron radiography systems to provide discrimination between various organic materials, systems using multiple neutron energy sources, together with detectors with the means for distinguishing between the different neutron energies have been proposed (Chen, G. and Lanza, R.C., 2000, Buffler, 2001). The key drawbacks of these systems have been their reliance on

35   complex, energy-discriminating neutron detectors and/or their use of sophisticated, high-energy accelerator-based neutron sources.

4

## Disclosure of Invention

In a first aspect, the invention is radiographic equipment comprising:

a source of neutrons;

a source of X-rays or gamma rays;

5       a collimated detector including:

an array of scintillators to receive radiation energy from the source of neutrons and the source of X-rays or gamma-rays having passed through an object, and to convert the received energy into light pulses;

a plurality of photo transducers optically coupled to respective scintillators

10  for converting the light pulses to charge pulses to produce an output signal; and

signal conditioning electronics to receive the output signal and generate output representing the interior of the object for visual display; and

a transport mechanism arranged to transport the object between the source of neutrons and the detector.

15

A sealed tube or other compact neutron generator may produce the neutrons and the radiographic equipment may utilise one or more neutron energies. In one example a single neutron source of 14 MeV may be produced via the deuteron-triton fusion reaction. In a further example, the radiographic equipment may utilise two tubes, one

20  to produce 14 MeV neutrons via the deuteron-triton fusion reaction and a second to produce 2.45 MeV neutrons via the deuteron-deuteron fusion reaction. The measurement of the neutron transmission at a second energy can be used to enhance the capability of the single energy transmission technique.

The source of X-rays or gamma-rays may comprise an X-ray tube, or an

25  electron linear accelerator to produce Bremsstrahlung radiation or a radioisotope source such as $^{60}$Co. The energy of the X-rays or gamma-rays will be sufficient to substantially penetrate through the object to be imaged.

The source of X-rays or gamma-rays and/or the source of neutrons may be housed within a source shielding provided with a slot such that the source of X-rays or

30  gamma-rays and/or the source of neutrons is collimated. The source shielding may be manufactured from thick paraffin, thick concrete, iron-shot concrete shielding blocks, or the like. Similarly, the detector may be housed within a detector shielding having a slot in order to provide the collimation. The collimation shielding may be made from iron and may have a thickness of between 100 mm and 250 mm. The width of the slot

35  may be selected to allow direct passage of neutrons and gamma rays from the source to the detector and to shield the detector array from scattered radiation. The detector slot

will be about the same width as the detector and the source collimator slots may be somewhat narrower.

The photo transducers may be photodiodes.

The scintillators used for X-rays or gamma rays may be separate from or the same as those used for neutrons.

The scintillators may be selected such that their spectral response is closely matched to the photodiodes. The scintillators may further be surrounded by a mask to cover at least a portion of each of the scintillators, each mask having a first reflective surface to reflect escaped light pulses back into the scintillator. The mask will have an opening to allow scintillator light to be detected by the photodiode.

The mask may comprise layers of PTFE tape and/or Tyvek paper. In one example, about five or six layers of PTFE tape may be used with three layers of Tyvek paper. In another example, about three layers of Tyvek paper may be used. Alternatively the mask may be painted onto the body of the scintillator.

Silicone oil, GE-688 grease, polysiloaxine, optical cement such as Eljen EJ-500 cement, or the like may be used to optically couple the photodiodes to the respective scintillators.

In one example, where the radiographic equipment comprises a single source of 14 MeV neutrons and a source of X-rays or gamma-rays, the scintillators may be plastic scintillators or liquid scintillators.

In a further example where the radiographic equipment comprises separate neutron and gamma-ray detectors, the gamma-ray scintillators may be plastic scintillators, liquid scintillators or inorganic scintillators such as caesium iodide, sodium iodide or bismuth germanate. Alternatively the X-ray or gamma ray detectors may be ionisation chambers.

In a further example where the radiographic equipment comprises dual neutron sources and a source of X-rays or gamma-rays, the scintillators may be plastic or liquid scintillators, preferably coupled to photomultiplier tubes.

The radiation receiving face of each scintillator, or the 'area' of each scintillator, corresponds to a single pixel. The area of each scintillator may typically be smaller than about 20 mm by 20 mm. Smaller areas lead to improved spatial resolution.

The thickness of each scintillator may be in the range 50 to 100 mm and may be a function of the detection efficiency and light collection efficiency. In an example where the object to be imaged is a unit load device or ULD such as those typically used in airport environments, the radiation receiving face of the array of scintillators may have dimensions of about 120 mm x 3300 mm and may comprise about 1000 pixels. When combined with a 14 MeV neutron source energy of approximately $10^{10}$

neutrons/second, the contents of a single ULD may be imaged over a time period of about one minute.

The signal conditioning electronics may include low noise and high gain amplifiers to amplify the output signals. A computer may be used to receive the
5 transmission outputs from the signal conditioning electronics, perform image processing and display the images to an operator on a computer screen.

As an object to be imaged is scanned, one or more outputs are obtained measuring the transmission of the 14 MeV neutrons through the object, the 14 MeV neutrons and X-ray or gamma-rays through the object, or the 14 MeV, 2.45 MeV
10 neutrons and X-ray or gamma-rays through the object. The detector may simultaneously detect more than one output.

Each of the source inputs may be separately processed. A scintillation spectrum may be collected separately for each pixel of the array to deduce neutron and X-ray or gamma-ray count rates for each pixel. The information may then be assembled to form
15 a complete 2-dimensional neutron image and a complete 2D X-ray or gamma-ray image. The resulting image may have a vertical resolution governed by the pixel size, and a horizontal resolution governed by the pixel size and the frequency with which the array is read out.

The computer may also be able to perform automatic material identification.
20 For instance, the transmission outputs may be converted to mass-attenuation coefficient images for each pixel for display on a computer screen with different pixel values mapped to different colours. In particular mass-attenuation coefficient images may be obtained from the count rates measured from the transmissions for each of the 14 MeV neutrons and X- or gamma-rays or the 14 MeV neutrons, 2.45 MeV neutrons and X- or
25 gamma-rays.

Analysis of the mass-attenuation coefficient images allows a variety of inorganic and organic materials to be distinguished. Such analysis may include forming cross section ratio images between pairs of mass attenuation coefficient images. Depending on whether a single or dual neutron sources are utilised, cross
30 section ratio images may be formed from the mass-attenuation coefficient images of the 14 MeV neutrons and the X- or gamma-rays, the 14 MeV neutrons and the 2.45 MeV neutrons, and the 2.45 MeV neutrons and the X- or gamma-rays. Advantageously, such images are independent of the mass of the object.

The proportions in which the cross section ratio images are combined may be
35 operator adjusted to maximise contrast and sensitivity to a particular object being examined in the image.

An image may be formed that is a linear combination of two cross section ratio images.

Two regions in an image may be identified which contain a first substance, but only one of the regions may contain a second substance. By performing cross section subtractions the image of the first substance may be effectively removed leaving the image of the second substance available for identification. The mass of the second substance may be obtained from the X- or gamma-ray transmission data.

In one example, the source of neutrons and the detector are stationary and the transport mechanism is arranged such that the object is moved in front of the source of neutrons and gamma rays. In a further example, the object may be stationary and the transport mechanism arranged such that the source and the detector move in synchronicity either side of the object. In a still further example, multiple sets of detectors may be situated around a centrally located radioactive source to allow scans of a plurality of separate objects to be acquired simultaneously. In such an example, the transport mechanism may be arranged such that the objects can be moved between the source of neutrons and the respective detector. Alternatively, the sources and detectors can be rotated around the object to be examined to allow multiple views to be obtained.

The rate at which the object is able to be moved in front of either the source of neutrons, or, the source of neutrons and X-rays or gamma-rays is partially dependent on the intensity of the neutron and gamma ray sources. The intensity of the single neutron source of 14 MeV may be in the order of $10^8$ neutrons/second, or $10^{10}$ neutrons/second, or as high as practically possible.

The rate at which the object is able to be moved in front of the source of neutrons and X-rays or gamma-rays is further dependent on the radiation receiving face of the array of scintillators and the number of scintillators. In addition, the length of the array is partially dependent on the length of the object to be imaged.

The object may be scanned between the neutron and gamma ray sources and detector and may pass through a shielded tunnel. The transport mechanism may comprise a pair of rails for the positioning of a dolly or platform on which the object may be transported. Alternatively, the transport mechanism may include a conveyor belt or other like arrangement for passing or winching objects through the tunnel. The transport mechanism may be automated such that the object is smoothly transported in front of the source of neutrons at a controllable uniform rate.

The invention may be applied to non-invasive examination of air cargo Unit Load Devices (ULD), or smaller containers or packages, the detection of contraband, explosives and other articles, substances and materials. It may provide improved specificity for contraband materials, such as organic materials in primarily inorganic

matrices, as well as the detection and identification of specific classes of organic material. It is particularly suited for the detection of explosives, narcotics and other contraband items concealed in aircraft baggage, airfreight containers and shipping containers.

5    It may also provide increased automation of the inspection process, with reduced reliance on human operators.

Further, it may provide a fast scanning rate so that a high throughput can be achieved. It is simple, low-cost and uses safe radiation sources; and simple, low-cost radiation detection systems. It may operate with a high detection rate and low false

10    alarm probability.


Brief Description of Drawings

Several examples of the invention will now be described with reference to the accompanying drawings, in which:

15    Figure 1 is a perspective view of the radiographic equipment;

Figure 2 is a bar graph of the calculated ratio, R, of a 14 MeV neutron to $^{60}$Co gamma-ray mass attenuation coefficients for a large number of benign, narcotic and explosive materials;

Figure 3 is a plot of the calculated ratio, R, of the 14 MeV neutron to the $^{60}$Co

20    gamma-ray mass attenuation coefficients for a range of elements;

Figure 4a is a display output of a gamma-ray scan of a motor bike, figure 4b is a display output in which the image is coloured according to the mass attenuation coefficient ratio, R, for 14 MeV neutrons and gamma rays;

Figure 5a is a schematic illustration of a selection of material samples and

25    common objects arranged on wooden shelves; Figure 5b is a display output of a gamma-ray scan; Figure 5c is a display output in which the image is coloured according to the mass attenuation coefficient ratio, R, for 14 MeV neutrons and gamma rays;

Figures 6a is a schematic illustration of a selection of material samples,

30    concealed contraband, alcohol, as well as simulated and real explosives; Figure 6b is a display output of a gamma-ray scan; Figure 6c is a display output in which the image is coloured according to the mass attenuation coefficient ratio, R, for 14 MeV neutrons and gamma rays;

Figures 7a is a photograph of a ULD containing assorted household electronics

35    metal items, concrete blocks and concealed contraband; Figure 7b is a display output of a gamma-ray scan; Figure 8c is a display output in which the image is coloured according to the mass attenuation coefficient ratio, R, for 14 MeV neutrons and gamma

rays; Figure 7d is the display output of figure 7c which has been further processed to emphasise the organic material;

Figure 8a is a photograph of a ULD containing assorted household items and concealed drugs, Figure 8b is a display output of a gamma-ray scan; Figure 8c is a display output in which the image is coloured according to the mass attenuation coefficient ratio, R, for 14 MeV neutrons and gamma rays R; Figure 8d is the display output of figure 8c which has been further processed to emphasise the organic material; and

Figure 9a is a photograph of a ULD containing assorted household items and concealed drugs, Figure 9b is a display output of a gamma-ray scan; Figure 9c is a display output in which the image is coloured according to the mass attenuation coefficient ratio, R, for 14 MeV neutrons and gamma rays; Figure 9d is the display output of figure 9c which has been further processed to emphasise the organic material.

## Best Mode for Carrying Out the Invention

Figure 1 illustrates the general layout of the radiographic equipment 10. The equipment 10 includes two separate generators of radiation, the first is an A-325 MF Physics neutron generator having a D-T neutron emitting module to produce a neutron energy source 12 having an energy of 14 MeV. The neutron generator is operated at a voltage of 80-110 kV. The second generator of radiation is a 0.82 GBq (or 22 mCi) $^{60}$Co source 14 to produce a source of gamma-rays and is located to the right of and adjacent to the neutron generator. The neutron generator and $^{60}$Co source 14 are situated within a source shield housing 16.

A 1600 mm long and 20 mm wide detector array 18 is situated in the vicinity of the radiation source and is housed in a detector shield housing 20. The detector array 18 is built up of eighty plastic scintillator rods (not shown), each with a radiation receiving area of 20 mm x 20 mm, and a length of 75 mm. The scintillator rods are made of an orange plastic scintillator in order to match the spectral response of the silicon photodiodes to the respective plastic scintillators. The photodiodes (not shown) are optically coupled to respective scintillators with optical cement. A reflective mask is painted on each of the orange scintillator rod and photodiode combinations to minimise the loss of any light that escapes the scintillator rods.

Since respective photodiodes have no internal gain, the signal conditioning electronics include preamplifiers used in conjunction with high-gain amplifiers in order to amplify the output signal for both neutrons and gamma-rays.

The equipment 10 accommodates a ULD 28 with a width up to 2.5 m and a height of 1.7 m. Each ULD 28 to be imaged is mounted on a platform 30 that has

runners to engage with a pair of tracks 32. In practice in an airport the ULDs could be scanned while still mounted on their respective dollies that are used to transport the ULDs around the airport. The ULDs and their dollies could be driven onto a platform that would traverse the radiation beams at a known speed. This would minimise the
5   handling of ULDs at the airport.

A further shield in the form of a tunnel 34 is provided. The tunnel 34 is sufficiently long enough so that the equipment can be operated without doors on either end. This permits the number of ULDs passing through the equipment 10 to be maximised.

10   Collimating slits (not shown) and cut into the source and detector shield respectively serve to define a fan shaped radiation beam, directed from the sources 12 and 14 towards the radiation detector 18. The detector collimating slit 38 and detector 18 extend the full height of the tunnel 34. Slots (not shown) in the sides of the shield 34 are provided and mate with collimating slits and for the passage of radiation from
15   the sources 12, 14 to the detector 18.

Each of the radiation shields 16, 20 and 34, attenuate and absorb both gamma rays and neutrons. Shielding materials used include concrete, iron and polyethylene. The radiation shields 16, 20 and 34 provide radiological protection for operators of the equipment or other persons in its immediate vicinity.

20   In operation, objects that are to be imaged are situated on the platform 30 that is then motorised through the tunnel 34. In the full-scale prototype scanner described here the platform 30 is typically operated at a speed such that each 10 mm increment takes approximately forty seconds to collect. This corresponds to a speed of 0.25 mm/sec; consequently, about 2½ hours are required to collect the image of a full ULD.
25   In practice, the speed at which the ULD travels through the equipment can be increased by a factor of over one hundred by increasing the intensity of the neutron source and by increasing the area of the detector array.

As the object passes through the tunnel 34, a scintillation spectrum is collected separately for each element of the 80-pixel array. These spectra are read out and reset
30   every time the platform 30 traverses 10 mm and the spectra are used to deduce neutron and gamma-ray count rates for each pixel. The information in each vertical strip is then assembled to form complete, 2-dimensional neutron and gamma-ray images.

The resulting image has a vertical resolution of 20 mm, governed by the pixel size, and a horizontal resolution of 10 mm, governed by the frequency with which the
35   80-pixel array is read out. As discussed below, deconvolution of the final image is performed to correct any blurring that may arise as a result of the combination of the motion of the platform 30 during the scan and the 20 mm width of the pixels.

Suppose that the neutron intensity and gamma-ray intensity transmitted though an object and detected in a particular pixel from each image are $I_n$ and $I_g$ respectively and that the neutron intensity and gamma-ray intensity transmitted and detected in a particular pixel from each image without an object present are $I_{on}$ and $I_{og}$ respectively.

5      Then the attenuation of fast neutrons through an object of density $\rho$ and thickness x can be calculated using the equation:

$$I_n/I_{on} = \exp(-\mu_{14}\,\rho\,x) \tag{1}$$

10      Similarly the attenuation of gamma ray attenuation through the object can be written as:

$$I_g/I_{og} = \exp(-\mu_g\,\rho\,x) \tag{2}$$

15  where $\mu_{14}$ is the neutron mass attenuation coefficient at 14 MeV and $\mu_g$ is the gamma mass attenuation coefficient. The mass attenuation coefficient ratio can then be calculated directly:

$$R = \mu_{14}/\mu_g = \ln(I_n/I_{on})\,/\,\ln(I_g/I_{og}) \tag{3}$$

20

Where R is directly related to the composition of the object and allows a wide variety of inorganic and organic materials and elements to be distinguished.

Figures 2 and 3 illustrate the ability of R to distinguish a wide variety of inorganic and organic materials. Natural materials that are primarily carbohydrate based such as cotton, paper, wood as well as many foods, protein based natural materials such as wool, silk and leather and synthetic organic materials - mainly polymers can be broadly distinguished. As illustrated, inorganic materials such as pottery, ceramics and metal items are easily distinguished from organic materials.

Due to the higher count-rates and lower background scattering of the gamma rays, the gamma-ray image carries most of the information about shape and density. For each pixel in the image, the quantity $\ln(I_g/I_{og})$ is calculated, which is proportional to the total mass per unit area of material along the line from the radiation source to the pixel in question. A "Mexican-hat" sharpening filter is applied to this image to improve object definition and reduce the effects of the motion and pixel-size blurring that affects the horizontal resolution of the image.

The pixel-by-pixel ratio of the neutron and gamma-ray images carries information about the average composition of each pixel, which is independent of the amount of intervening material.

Due to the relatively low counting statistics in the neutron image, there is considerable pixel-to-pixel noise present in the composition image. Consequently, a 5×5-pixel Gaussian smoothing filter is applied to this image. Whilst this reduces the resolution of the composition information in the final image, it significantly enhances the visibility of subtle changes in composition for objects with dimensions of more than about 50 mm.

The results from six scans are shown in figures 4 to 9. The gray-scale images illustrate the results of the gamma-ray scan alone and as such show the results that would be achievable from a conventional X-ray scanner. Regions with little or no intervening material show as white and denser materials show as darker shades of grey. The colour images combine the gamma-ray shape and density information, together with the composition information from the neutron/gamma ratio image. The density of colour shows the material density with white corresponding to no intervening material and denser regions having a saturated colour. The colour of a pixel corresponds to the R value for that pixel, with lower R values coloured blue, intermediate values turquoise through green to yellow and higher values orange. The exact mapping between R value and colour is different for each image, with the colour scale adjusted to show the maximum information in each case. For the ULD scans, an enhanced organic image is also presented. This emphasises organic regions of the image, which are coloured yellow, orange and red.

Figure 4a illustrates the result of the gamma ray scan alone of a motorbike. Figure 4b illustrates the combined gamma-ray shape and density information together with the composition information from the neutron/gamma ratio image scan of a motorbike. This image provides a good indication of the overall imaging capabilities of the equipment. In particular, fine details such as the front brake cables 52 show quite clearly in figure 4b, even though they are considerably smaller than the 20 mm pixel size. The metal frame 54 and engine 56 of the bike show up blue in figure 4b; whereas the fuel 58 in the petrol tank, rubber tyres 60, plastic seat 62 and lights show up orange. The oil 64 in the sump (immediately above the kickstand), when averaged together with the metal around it shows as a green patch. In contrast, from the conventional gamma-ray image Figure 4a, it is difficult or impossible to distinguish between the oil 64 and the sump.

Figures 5a to 5c illustrate a selection of material samples and common objects arranged on wooden shelves. Again, metals such as iron 66, lead 68 and aluminium 70

show up dark-blue. Intermediate materials such as concrete 72, glass 74 (in the computer monitor 75) and ceramic powder (alumina, $Al_2O_3$) 76 show up lighter blue. Finally, the organic materials, including elemental simulants of heroin 77, methamphetamine 78, cocaine 80 and TNT 82 show up in a variety of colours from
5   green to orange, depending on the R value of the material. Two ceramic statues on the top shelf, one filled with iron shot 84 and the other with sugar 86 can be clearly distinguished, both by density and by composition.

Figure 6a to 6c illustrate a further selection of materials, including concealed contraband, alcohol and both simulated and real (Detasheet) explosives. Three hollow
10   concrete blocks are positioned on the top shelf. The left-hand block contains concealed organic material 94 (drug substitute); the centre block is empty and the right hand block contains alumina powder 96. These three blocks provide simple models of drugs concealed within a ceramic or pottery object, a hollow, empty object and a hollow, empty object with thickened walls. Whilst the gamma-ray image of figure 6b clearly
15   distinguishes between the empty 95 and filled blocks 94 and 96, it cannot separate the drug-surrogate filled block 94 from the alumina filled block 96. In contrast, the neutron image of figure 6c clearly reveals the concealed organic filling 94. On the left hand side of the middle shelf are positioned two containers, one filled with pure alcohol 98 (Meths) and one with water 100 ($H_2O$). The alcohol 98 shows clearly as being more
20   'organic' (higher R value) and is predominantly orange in colour; the water 100, with a lower R value is predominantly green. On the same shelf, the simulated 102 and real 104 explosives show as the same colour showing that the simulant is a good substitute for real explosive. On the bottom shelf is a case containing twelve glass bottles, six filled with simulated spirits 106 (40% ethanol, 60% water) and six filled with water
25   108. Again, the alcohol filled bottles 106 show up as having a higher R value (more green/orange) than the water 108 (predominantly blue).

Figures 7a to 7d, 8a to 8d and 9a to 9d illustrate the results of imaging ULDs filled with a variety of objects. In all three images, the filling of the ULD has been deliberately kept fairly simple, to simplify discussion of the results obtained. In
30   particular, most of the packing material that would normally be present (cardboard boxes, foam, polystyrene etc) has been omitted so that the objects in the ULD can be clearly seen. It is recognised that in reality, most ULDs would be considerably more cluttered.

Figures 7a to 7d illustrates a ULD filled with a variety of household electronics
35   (a refrigerator 120 and several computers 122), metal parts, hollow concrete blocks 124 (substituting for ceramic pipes or hollow statues or figurines) and tools. Two packets of plastic beads, substituting for drugs 126, are concealed within one of the computers

and inside one of the concrete blocks. A propane gas cylinder 128 is also hidden inside the ULD. Figure 7a illustrates a photograph of the ULD scanner. Figure 7b shows the results of the gamma-ray scan only. Neither of the packets of surrogate drugs are particularly obvious. The propane gas cylinder 128 can be identified on the basis of its

5   shape, although the organic nature of its contents is not clear. Figures 7c and 7d are coloured according to the neutron/gamma ratio R, as a result the inorganic materials show blue and the organic materials as orange. The proportions in which the two images are combined are adjusted by the operator to maximise contrast and sensitivity for organic materials which are coloured yellow and red and to minimise the effects of

10  clutter resulting from overlapping objects, the result is illustrate in figure 7d. Clearly both packets of concealed drugs 126 can be identified.

Figures 8a to 8d illustrates a ULD with drugs 124 concealed inside two computers 122 and a fridge 120. Whilst it can be seen in the gamma-ray image of figure 8b that the top two computers 122 appear somewhat different from the bottom

15  two, it is not clear whether this is a genuine difference in the structure of the machines. However, in the figures of 8c and 8d it is immediately apparent that the difference is due to a large volume of organic material, as shown by the bright orange colour of these regions. The top two computers 122 contain ~1 kg bags of plastic beads simulating packaged drugs. This is in contrast to the predominantly blue (inorganic or

20  low R value) colour of the rest of the computer structure 126. Similarly, it is not clear from the gamma-ray image of figure 8b of the fridge 120 whether the anomaly in the centre of the image is part of the structure of the fridge or not. However, in figures 8c and 8d it can be seen that the anomaly is clearly organic and in contrast to the predominantly inorganic structure visible in the rest of the fridge (in particular, the

25  compressor at the lower right and the freezer compartment at the top). Again, in the enhanced organic image of figure 8d the concealed drugs 124 are clearly visible. Additionally, other organic material in the ULD (notably the wooden shelving 128 behind the fridge 120 and the container of water to the left of the fridge 120) also shows up.

30      Figures 9a to 9d illustrate a second ULD with real concealed drugs (1 kg each of heroin and methamphetamine). The heroin 130 is hidden inside a hollow concrete block 132. The methamphetamine 134 is hidden inside a small box, which is placed inside a larger box 136 filled with clothing. The organic nature of the concealed drugs is evident from the colouring in the composition images of figures 9c and 9d. Once

35  again, the enhanced organic image of figure 9d effectively reveals the concealed drugs 130 and 134, especially the heroin 130 inside the concrete blocks 132. As the methamphetamine 134 is concealed within the box 136 of clothing (immediately

behind the front fork of the bicycle 140), composition discrimination is less revealing in this case. However, the package of drugs 134 can be identified as a potential anomaly on the basis of its shape and higher density.

The radiographic equipment as described can be used in at least three ways for detecting and identifying contraband materials. Firstly, the gamma-ray images provide considerable information about the shapes, sizes and densities of objects inside an object such as a ULD. Some suspicious materials can be identified on this basis. Particular examples would be packets of drugs concealed inside spaces or cavities of hollow objects. Secondly, the colouring of the gamma-ray image on the basis of composition information derived from the neutron measurements provides powerful extra clues in the interpretation of scan images and identification of suspicious materials. In particular, the detection of organic materials inside predominantly inorganic objects is greatly facilitated. Thirdly, under certain circumstances, the equipment can be used to measure the neutron/gamma ratio (R values) of suspicious materials to further assist in their identification. This approach works best when there is little over- or under-lying material around the substance being measured, or when the over- and under-lying material is reasonably uniform in the immediate vicinity of the measurement region. Under these circumstances, it is possible to make an approximate correction for the absorption of neutrons and gamma rays in the over- and under-lying material to obtain the R value of just the substance of interest.

It will be appreciated by persons skilled in the art that numerous variations and/or modifications may be made to the invention as shown in the specific embodiments without departing from the spirit or scope of the invention as broadly described. The present embodiments are, therefore, to be considered in all respects as illustrative and not restrictive.

DATED this twenty-ninth day of August 2003

Commonwealth Scientific and Industrial Research Organisation
Patent Attorneys for the Applicant:

F.B. RICE & CO.

# REFERENCES

An, J., Xiang, X., Wu, Z., Zhou, L., Wang, L. and Wu, H., "Progress on developing $^{60}$Co container inspection systems", Applied Radiation and Isotopes 58 (2003) 315-320

5   Bartle, C.M., "Method and apparatus for detecting concealed substances", US Patent 5,479,023 (Dec. 26, 1995)

Barzilov, A.P., Womble, P.C. and Vourvopoulos, G., 2001. "NELIS – a neutron elemental analysis system of commodities of pallets", 2001 Office of National Drug
10   Control Policy International Symposium

Brzosko, J.S. et al, "Advantages and limitations of 14-MeV neutron radiography", Nuclear Instruments and Methods B72 (1992) 119-131

15   Buffler, A., 2001. "Contraband detection by fast neutron scattering", 2$^{nd}$ National Nuclear Technology Conference, NAC, South Africa, 13-15 May 2001, paper D-03

Chen, G. and Lanza, R.C., 2000. "Fast neutron resonance radiography for elemental mapping", Final Research Co-ordination Meeting on "Bulk Hydrogen Analysis using
20   Neutrons", Cape Town, South Africa, 23-26 October 2000, pp. 31-38

Dokhale, P.A., Csikai, J., Womble, P.C. and Vourvopoulos, G., "NELIS – an illicit drug detection system", AIP Conference Proceedings, 576 (2001) 1061-1064

25   Gozani, T., 1997. "Neutron based non-intrusive inspection techniques", Proc. Internat. Conf: On Neutrons in Research and Industry, Crete, Greece, 9-15 June 1996, SPIE Proceedings Series 2867 (1997) 174-181

Klann, R.T., 1996. "Fast neutron (14.5 MeV) radiography: a comparative study", 5$^{th}$
30   World Conference on Neutron Radiography, Berlin, 17-20 June 1996, 469 – 483.

Lefevre, H.W, et al, 1997. "Using a fast neutron spectrometer system to candle luggage for hidden explosives", Proc. Internat. Conf. On Neutrons in Research and Industry, Crete, Greece, 9-15 June 1996, SPIE Proceedings Series 2867 (1997) 206-210
35

Le Tourneur, P., Bach, P. and Dance, W.E., 1998. "Neutron fan beam source for neutron radiography purpose", 15th Int. Conf. on Applications of Accelerators in Research and Industry,Denton, Texas, USA, Nov. 4-7, 1998

5 Millen, M.J., Rafter, P.T., Sowerby, B.D., Rainbow, M.T. and Jelenich, L., 1990. "Plant trial of a fast neutron and gamma-ray transmission gauge for the on-belt determination of moisture in lump coke", Nuclear Geophysics 4 (1990) 215-226

Mikerov, V.I. et al, 2000. "Investigation of prospects of fast neutron radiography on the 10 basis of portable equipment", IAEA Coordinated Research Programme on "Bulk Hydrogen Analysis using Neutrons", Cape Town, South Africa, 23-6 October 2000, Report F1-RC-655.3

Rynes, J. et al, "Gamma-ray and neutron radiography as part of a pulsed fast neutron 15 analysis inspection system", Nuclear Instruments and Methods A422 (1999) 895-899

Sawa, Z.P., Gozani, T. and Ryge, P., 1991. "Contraband detection system using direct imaging pulsed fast neutrons", US patent No. 5,076,993, Dec. 31 1991

20 Tickner, J.R. and Sowerby, B.D., 2002. "A Detection System", Australian Provisional Patent Application No. 2002953244, Filing Date: 10 December 2002
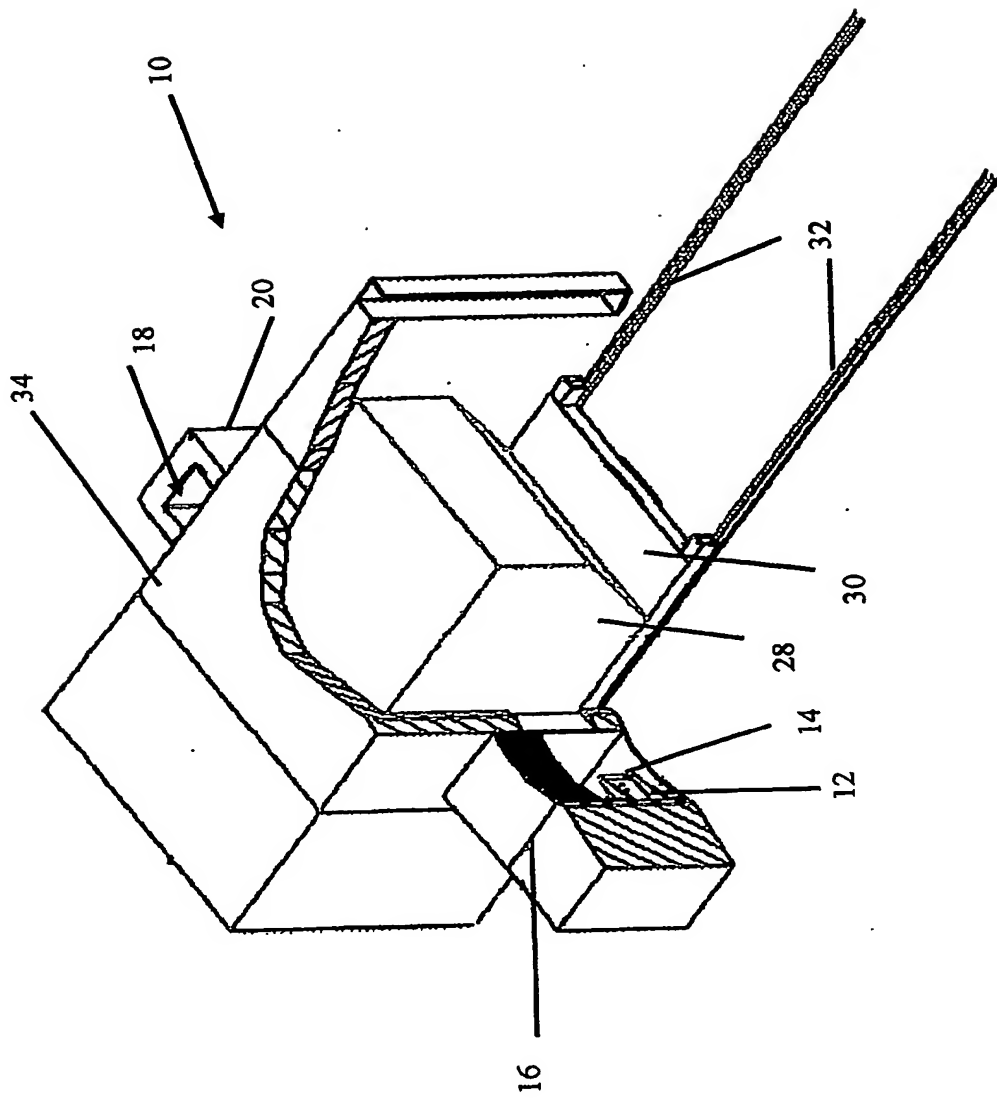
Fig. 1
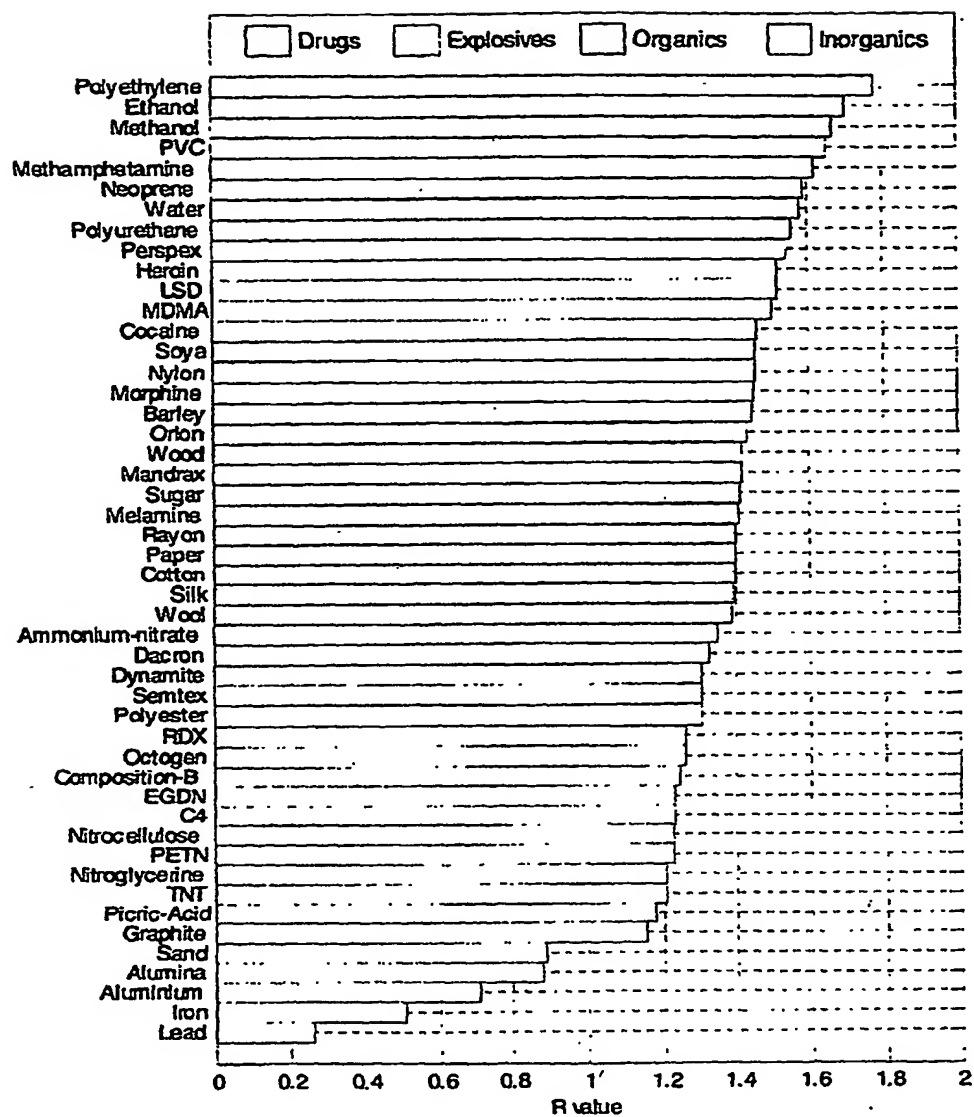
Fig. 2
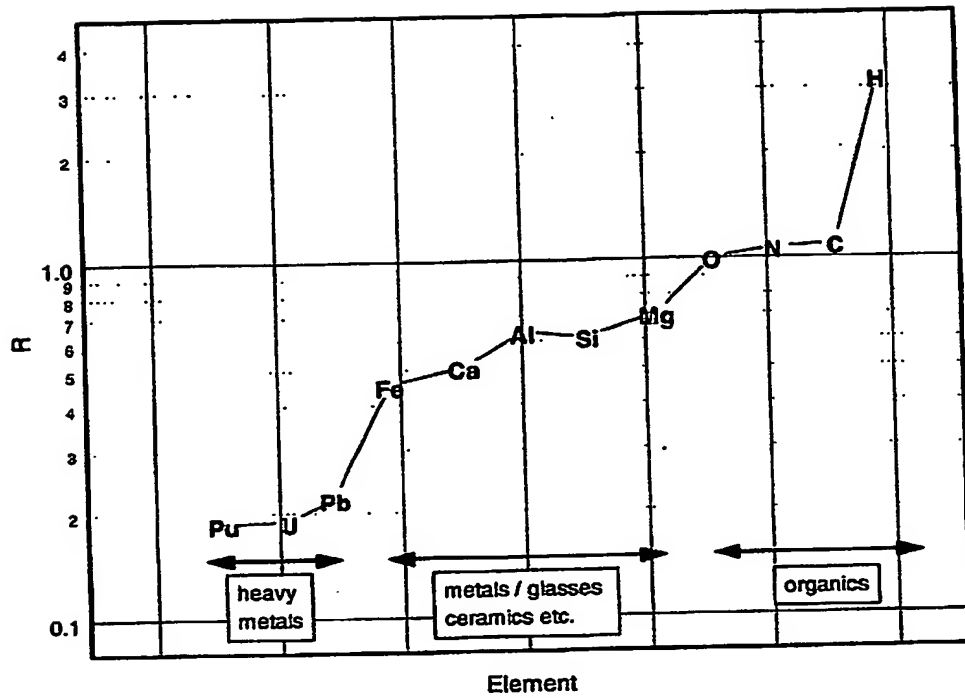
Fig. 3
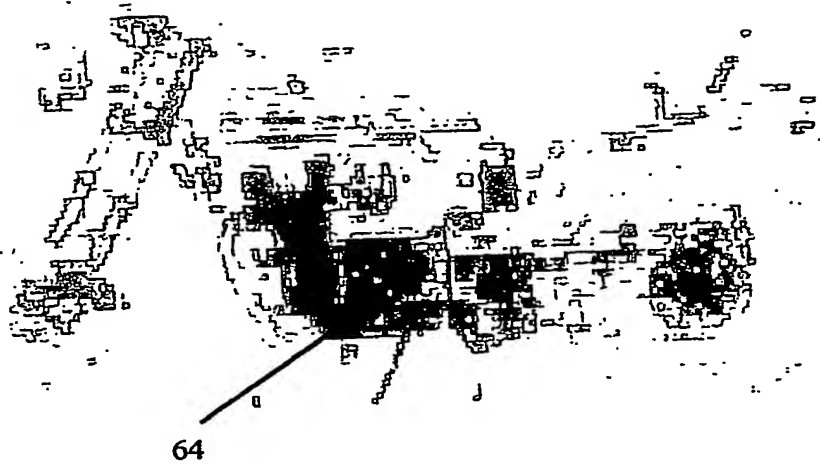
Fig. 4a



Fig. 4b

Fig. 5a



Fig. 5b



Fig. 5c

Hollow concrete blocks

Poly    Al₂O₃    Pb

98    Meths    Water    TNT    Detasheet

Fig. 6a

Spirits  Water    Kero-sene    Fe

Tungsten

95    96

94

Fig. 6b

96

94

98    104    102    Fig. 6c

100

106    108

Fig. 7b

Fig. 7d

124

124

126

128

120

126

128

122

124

124

Gas128
cylinder

Surrogate
drugs126

120

126

Surrogate
drugs 126

128

122

120

126
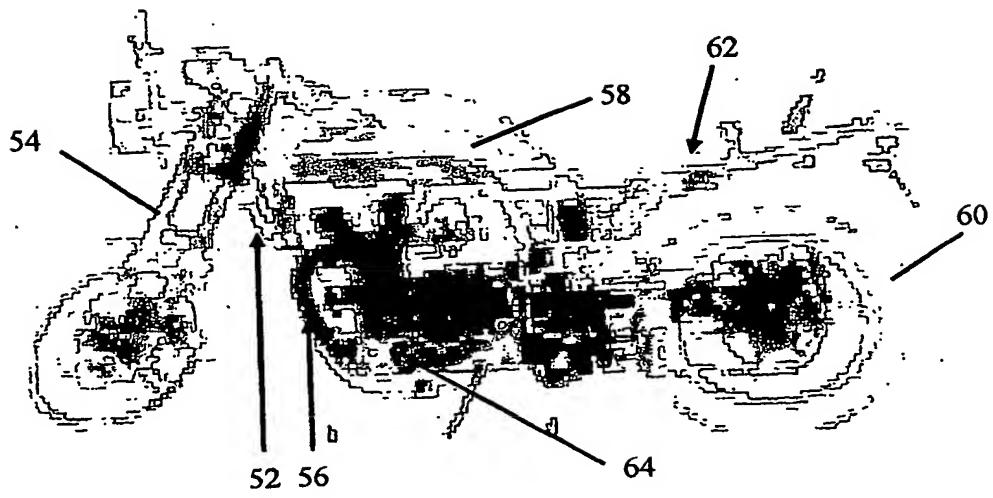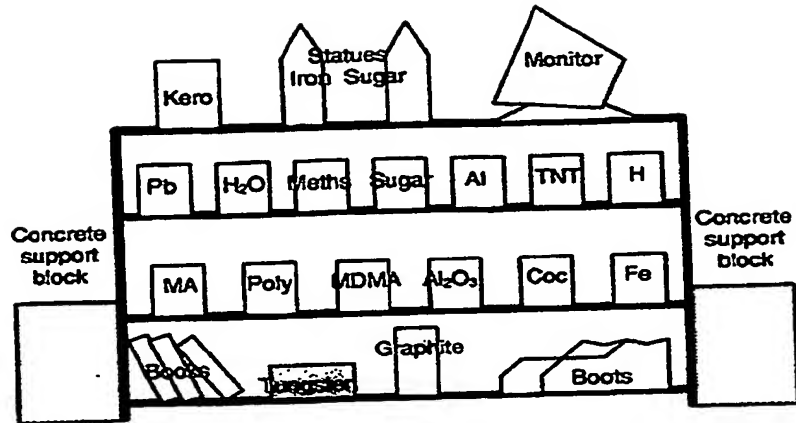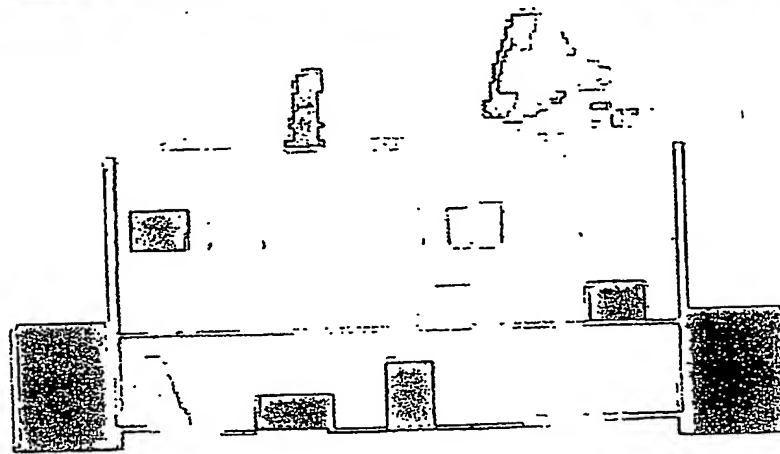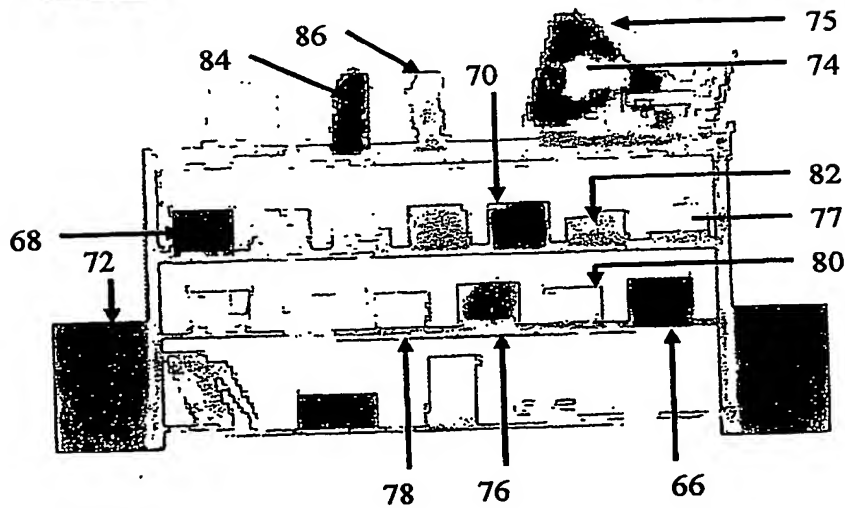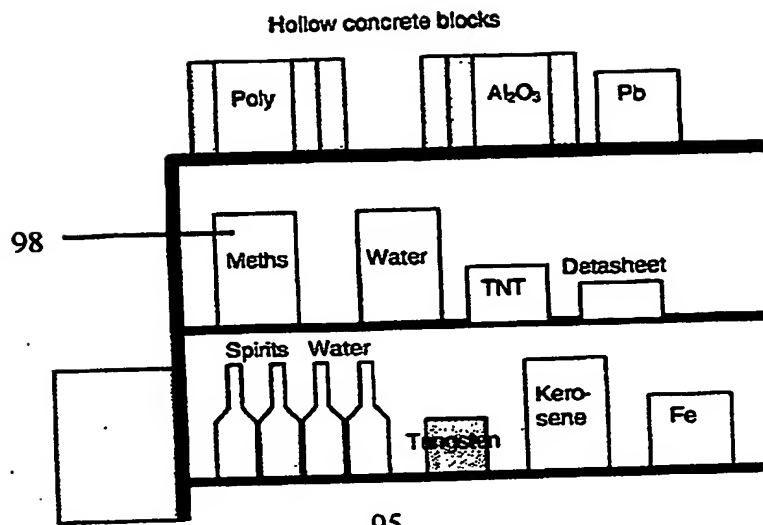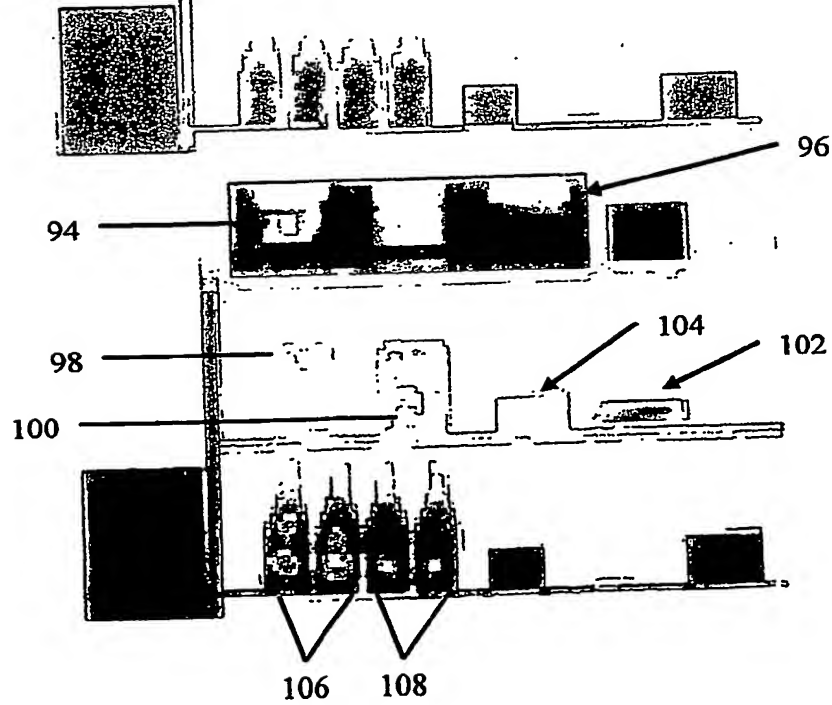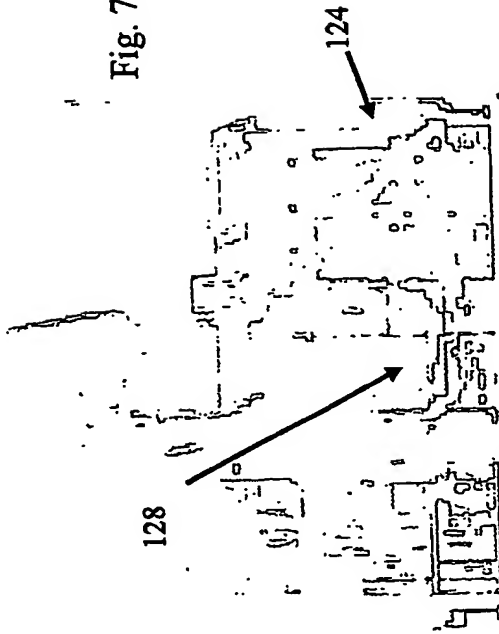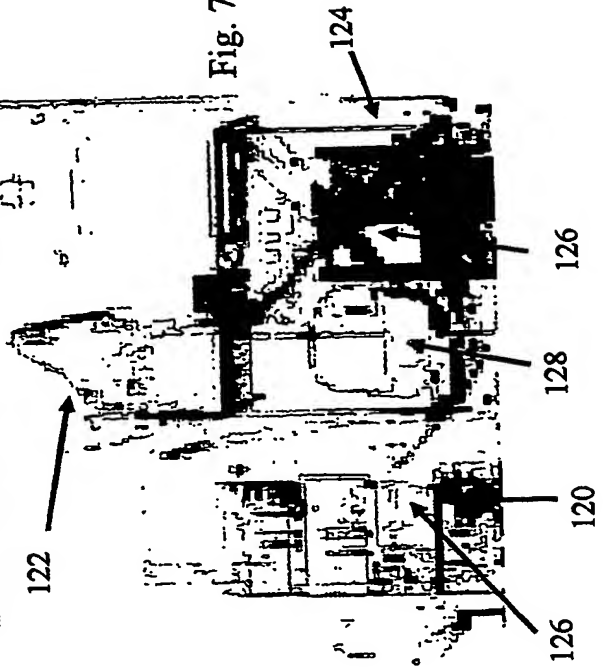
Fig. 7a
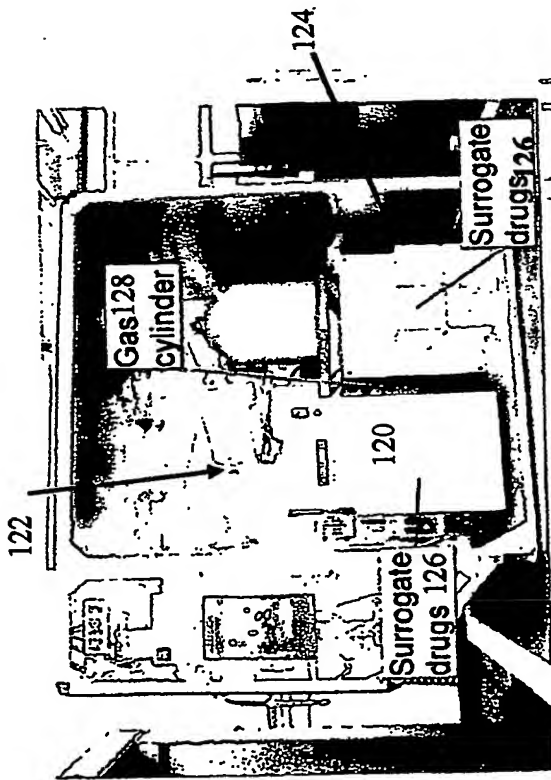
Fig. 7c

Fig. 8b

Fig. 8d

Fig. 8a

Fig. 8c

9/9

Fig. 9a

Fig. 9b

Fig. 9c

Fig. 9d

130

132

134

136

138

140